



**Internal Heavy-Atom Effect in 3-Phenylselanyl and 3-Phenyltellanyl BODIPY Derivatives Studied by Transient Absorption Spectroscopy**

Journal:	<i>Photochemical &amp; Photobiological Sciences</i>
Manuscript ID	PP-ART-10-2015-000366.R1
Article Type:	Paper
Date Submitted by the Author:	03-Dec-2015
Complete List of Authors:	Al Anshori, Jamaludin; Masaryk University, Department of Chemistry Slanina, Tomas; Masaryk University, Department of Chemistry Palao, Eduardo; Masaryk University, Department of Chemistry Klan, Petr; Masaryk University, Department of Chemistry

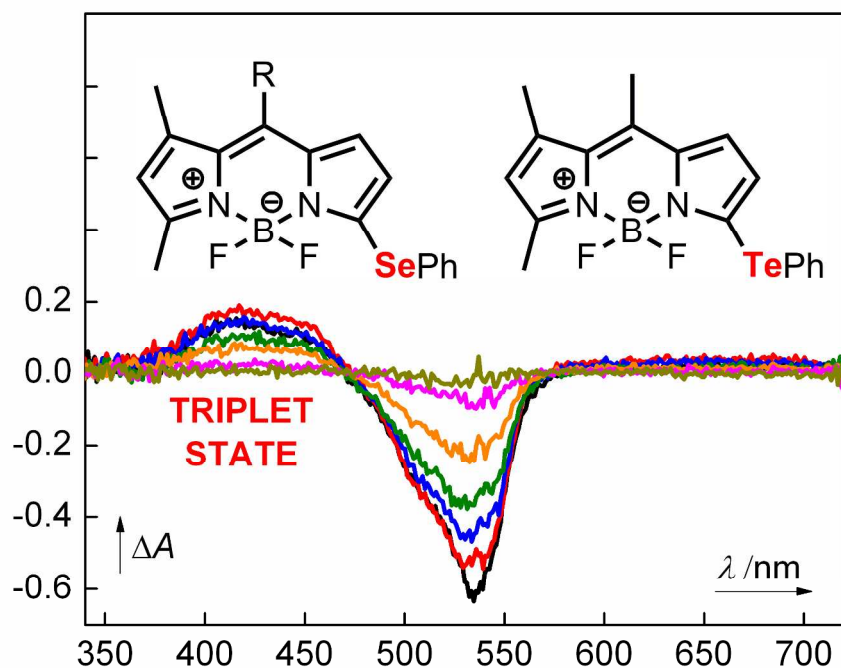
## Internal Heavy-Atom Effect in 3-Phenylselanyl and 3-Phenyltellanyl BODIPY Derivatives Studied by Transient Absorption Spectroscopy

Jamaludin Al Anshori, Tomáš Slanina, Eduardo Palao, Petr Klán\*

RECETOX, Faculty of Science, Masaryk University, Kamenice 5, 625 00, Brno

\* E-mail: klan@sci.muni.cz; Phone: +420-54949-4856; Fax: +420-54949-2443

Graphical abstract :



The extent of intersystem crossing related to the heavy-atom effect of the Se and Te atoms was investigated on monosubstituted 3-phenylselanyl and 3-phenyltellanyl BODIPY derivatives.

## Abstract

Three monosubstituted 3-phenylselenanyl and 3-phenyltellanyl BODIPY derivatives were synthesized and their spectroscopic properties were characterized and compared to those of iodine and chlorine-atom containing analogues as well as an unsubstituted BODIPY derivative. The fluorescence quantum yields were found to decrease, whereas the intersystem crossing quantum yields ( $\Phi_{ISC}$ ), determined by transient spectroscopy, increased in the order of the H→Cl→Se/I→Te substitution. The maximum  $\Phi_{ISC}$ , found for the 3-phenyltellanyl derivative, was 59%. The results are interpreted in terms of the internal heavy-atom effect of the substituents.

## Introduction

4,4-Difluoro-4-bora-3a,4a-diaza-*s*-indacene (BODIPY) derivatives have found extensive applications as fluorescent dyes and biological probes due to their robust and easily tunable photophysical properties.<sup>1-8</sup> BODIPY chromophores typically exhibit very high quantum yields of fluorescence; the intersystem crossing (ISC) quantum yield in most derivatives is negligible. This prevents their use as triplet photosensitizers in photocatalysis, photovoltaics, photodynamic therapy (singlet oxygen generation), or triplet–triplet annihilation upconversion.<sup>9</sup>

Nagano and his collaborators were first to prepare a 2,6-diiodo BODIPY derivative.<sup>10</sup> The presence of the iodine atoms enhances intersystem crossing due to a strong spin-orbit coupling between singlet and triplet states (heavy atom effect).<sup>11, 12</sup> High photoinduced cytotoxicity of this compound redirected the investigations, and various bromo and iodo analogues bearing different substituents<sup>5</sup> as well as those with alternative ISC promoters, such as heavy metal containing units, were designed and studied.<sup>6, 13, 14</sup> Such structural variations improved the physico-chemical properties of the chromophores and their cytotoxicities only in some cases.<sup>5, 15</sup> Heavy atom-free BODIPY dimers represent an alternative solution in the design of triplet sensitizers.<sup>16-20</sup> Structural variations of this type as well as extension of the BODIPY  $\pi$ -system by styryl or thiophene substituents shifts the absorption band maxima bathochromically to the NIR tissue transparency window (over 650 nm).<sup>21</sup> Several aza-BODIPY analogues have also been introduced as triplet photosensitizers.<sup>5</sup>

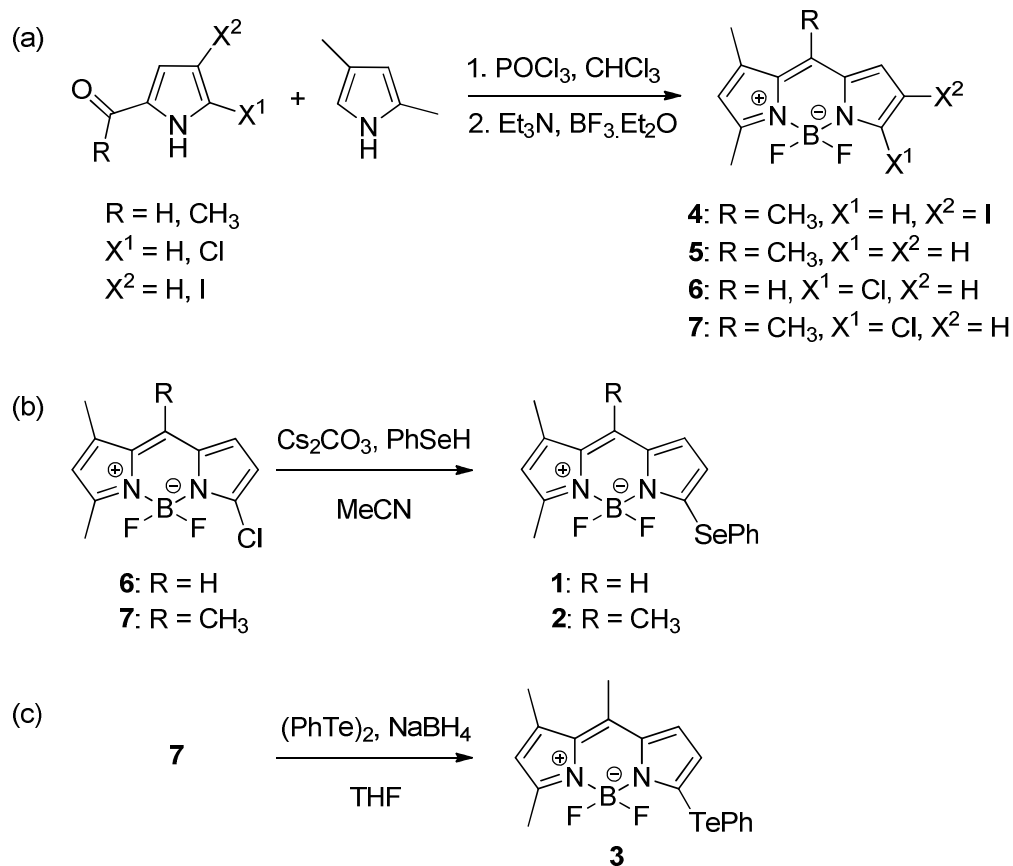
Important advances in the chemistry of selenium- and tellurium-containing organic compounds have been made in the past years due to their promising pharmacological properties and low toxicity.<sup>22-24</sup> These compounds can be used for sensing of reactive oxygen species (ROS), reactive nitrogen species (RNS), and bioorganic thiols.<sup>25-27</sup> Several examples of Se- and Te-BODIPY ROS sensors, based on turning off-on fluorescence in different oxidation states, have been reported.<sup>28, 29</sup> In most of these examples, the Se- and Te-atom containing groups are separated from the BODIPY chromophore by a linker that still permits an efficient intramolecular charge-transfer (ICT) in their reduced form. As far as we know, only two studies

describe the synthesis of compounds that have either Se or Te directly attached to the BODIPY core.<sup>30, 31</sup> In one of those works, Vosch and coworkers used transient spectroscopy and fluorescence single-photon timing experiments to conclude that the presence of one or two of these atoms dramatically reduces the fluorescence due to efficient ISC.<sup>30</sup> The triplet lifetimes and ISC quantum yields have not been determined. In addition, the authors suggested that ICT from chalcogen to the BODIPY core can be responsible for deactivation of the locally excited state.

In this work, we present the synthesis and spectroscopic characterization of several novel 3-phenylselanyl and 3-phenyltellanyl BODIPY derivatives. Transient absorption spectroscopy was used to determine the triplet lifetimes and ISC quantum yields to evaluate the effect of chalcogen substituents as heavy atoms. The spectroscopic results are compared to those obtained with some other reference BODIPY derivatives.

## Results

**Synthesis.** The 3-phenylselanyl BODIPY derivatives **1** and **2** were synthesized from the corresponding chlorides **6** and **7**, prepared by the condensation of two pyrrole derivatives according to Dehaen and coworkers<sup>32</sup> (Scheme 1a; see also Experimental Part), via an S<sub>N</sub>Ar reaction of benzeneselenolate generated from benzeneselenol and Cs<sub>2</sub>CO<sub>3</sub> in good chemical yields (~70%; Scheme 1b), analogous to the procedure of Vosch and coworkers.<sup>30</sup> The 3-phenyltellanyl BODIPY derivative **3** was obtained from **7** and benzenetelluroolate generated from diphenyl ditelluride in the presence of NaBH<sub>4</sub> in 68% (Scheme 1c). The BODIPY derivatives **4** and **5** were again synthesized using a method<sup>32</sup> (Scheme 1a) described above in 65 and 14% yields, respectively.



**Scheme 1.** Synthesis of the BODIPY Derivatives **1–7**.

**Photophysical Properties.** The absorption spectra of the BODIPY derivatives **1–7** in acetonitrile possess a major absorption band ( $\lambda_{\text{max}}$ ) in the region of 483–540 nm (Figure 1, Table 1). The absorption bands are bathochromically shifted for the derivatives **1–3** compared to those of **4–7**. Their values are affected by the solvent polarity (Figure S1; aggregation of **1** was excluded in a concentration dependence study, Figure S2). For example,  $\lambda_{\text{max}}$  of **1** in water is 540 nm, and a new shoulder appears at 576 nm (Figure S1). The compounds **5–7** exhibit bright fluorescence, whereas the heavy atom (I, Se, Te) containing derivatives **1–4** are only weakly fluorescent at room temperature (Figure 2; Table 1). A higher signal-to-noise ratio in the emission signal of **3** is a consequence of its very low fluorescence quantum yield,  $\Phi_f$ . The bathochromic shifts caused by the heavy atoms in the absorption spectra of **1–3** are also apparent in their emission spectra. The fluorescence lifetimes,  $\tau_f$ , of **1**, **2** and **4** were shorter than those of the BODIPY derivatives **5–7**. We were unable to determine  $\tau_f$  of **3** because the compound photochemically degraded during the fluorescence measurement, and a new signal of a photoproduct overlapped that of **3** (see also below).

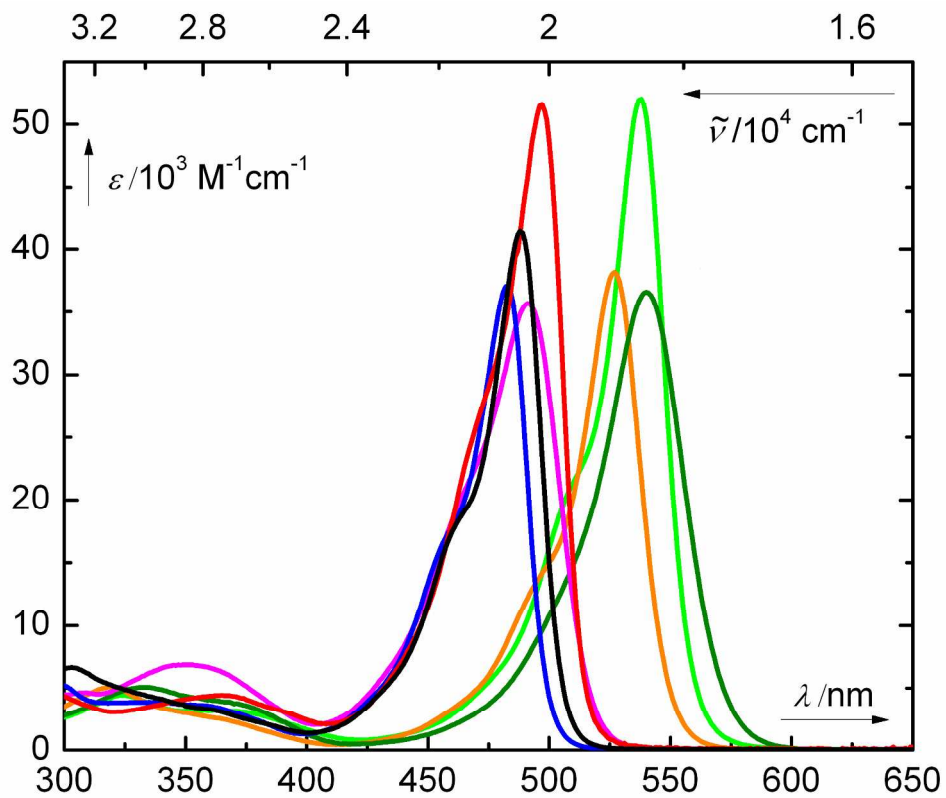


**Figure 1.** Absorption spectra of **1–7** in acetonitrile (**1**: light green; **2**: orange; **3**: dark green; **4**: magenta; **5**: blue; **6**: red; **7**: black).

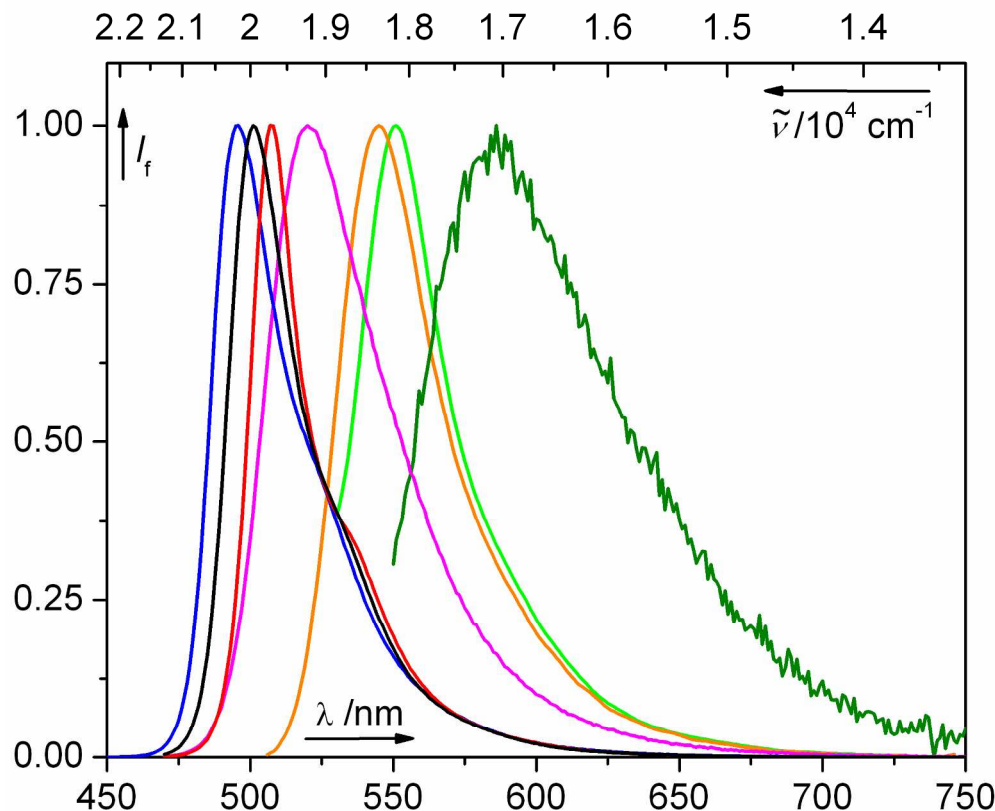


**Figure 2.** Normalized emission spectra of the BODIPY derivatives **1–7** in acetonitrile (**1**: light green; **2**: orange; **3**: dark green; **4**: magenta; **5**: blue; **6**: red; **7**: black).

**Table 1.** Absorption Photophysical Properties of **1–7** in Acetonitrile

compound	$\lambda_{\max}/\text{nm}$	$\epsilon_{\max}^a$	$\lambda_f/\text{nm}^b$	$\Delta\tilde{\nu}/\text{cm}^{-1}^c$	$\Phi_f/\%$ <sup>d</sup>	$\tau_f/\text{ns}^e$
<b>1</b>	538	52000	551	438	$6.3 \pm 0.4$	$0.53 \pm 0.01$
<b>2</b>	527	38200	540	457	$20 \pm 1$	$1.23 \pm 0.01$
<b>3</b>	540	36600	585	1224	$0.09 \pm 0.03$	n. d. <sup>g</sup>
<b>4</b>	493	35400	520	1053	$4.8 \pm 0.2$	$0.34 \pm 0.01$
<b>5</b>	483	37100	496	543	$92 \pm 3$	$5.98 \pm 0.01$
<b>6</b>	497	51640	507	397	$74^f$	$5.46 \pm 0.01$
<b>7</b>	488	37840	501	532	$73^f$	$5.60 \pm 0.01$

<sup>a</sup>  $\epsilon_{\max}/\text{mol}^{-1} \text{ dm}^3 \text{ cm}^{-1}$ . <sup>b</sup> **1**:  $\lambda_{\text{exc}} = 510 \text{ nm}$ ; **2**:  $\lambda_{\text{exc}} = 450 \text{ nm}$  (the emission signal of **5** as an impurity (photoproduct) was subtracted from the spectrum); **3**:  $\lambda_{\text{exc}} = 540 \text{ nm}$ ; **4**, **6** and **7**:  $\lambda_{\text{exc}} = 460 \text{ nm}$ ; **5**:  $\lambda_{\text{exc}} = 440 \text{ nm}$ . <sup>c</sup> The Stokes shift. <sup>d</sup> The standard deviations were calculated from 5 independent measurements. <sup>e</sup> The standard deviations were calculated from 3 independent measurements. <sup>f</sup> From the ref. 33. <sup>g</sup> n. d. = not determined.

**Chemical Stability.** The compounds **1–5** were found to be stable when kept in acetonitrile solutions ( $c = 1–3 \times 10^{-5} \text{ mol dm}^{-3}$ ) in the dark at 22 °C. Their concentrations decreased only by 3–4% in 10 days. When the solutions were irradiated at 525.5 nm, the Se-BODIPY derivatives **1** and **2** were found to be more stable than the Te- and I-analogues **3,4** (Table 2). The compound **5** was the most photostable of all studied derivatives. Upon irradiation of **1–3**, a new emission band at ~496 nm appeared (Figures S3–S5). The photoproduct **8**<sup>34</sup> (for absorption and emission spectra see Figure S20) was found to be formed from **1**, whereas the compound **5** was identified using HPLC (the authentic compound was used as a reference) as a photoproduct of the photolysis of **2** and **3** (Figure S21). As the compounds **5** and **8** have substantially higher fluorescence quantum yields than those of **1–3**, even trace amounts gave strong emission signals, which could be removed by spectral subtraction.

**Table 2.** Relative Photostability of **1–5** in Acetonitrile<sup>a</sup>

compound	$\tau_{1/2}/\text{h}$
<b>1</b>	24
<b>2</b>	101
<b>3</b>	0.2
<b>4</b>	7.7
<b>5</b>	650

<sup>a</sup> Irradiated using 32 high-energy LEDs (100 mW) emitting at  $\lambda_{\text{em}} = 525.5 \text{ nm}$  at the distance of ~1 cm from the cuvette window. The absorbance of the solutions at  $\lambda = 525.2 \text{ nm}$  were in the range of 0.1 and 1.0; the half-lives ( $\tau_{1/2}$ ) are recalculated for the same initial sample absorbance.

**Transient Spectroscopy.** Transient absorption spectra of **1** obtained 8 ns–50  $\mu\text{s}$  after excitation at 532 nm were measured in both aerated and degassed acetonitrile ( $c = 1.10 \times 10^{-5} \text{ mol dm}^{-3}$ ; Figures 3 and S6). Absorption maxima at 418 and ~650 nm as well as a ground-state bleach at 535 nm, resembling its absorption spectrum (Figure 1), were observed. The decay or rise of the signals at the corresponding wavelengths followed the same monoexponential kinetics, and we attribute the signals at 418 and ~650 nm to the lowest triplet state of **1**. Similar transient absorption of the triplet state of BODIPY derivatives has been reported before.<sup>30, 35</sup> A representative kinetic trace of the triplet state of **1** in both aerated and degassed acetonitrile solutions (Figure 4) gave the triplet lifetimes of  $\tau_{\text{T}} = 0.24$  and 7.3  $\mu\text{s}$ , respectively (Table 3). Transient spectra of the analogue **2** in both aerated and degassed acetonitrile solutions are shown in Figures S7 and S8. The absorption maximum ( $\lambda_{\text{max}}^{\text{T}} = 435 \text{ nm}$ ) and that of the ground state bleach at 520 nm are similar to those of **1**. A weak absorption band in the red part of the spectra seems to be somewhat shifted to longer wavelengths (Figures S6 and S7). The decay measured at the corresponding wavelengths followed the same monoexponential kinetics (Table 3). As the transient lifetime increased considerably (from  $\tau_{\text{T}} = 0.24$  to 7.1  $\mu\text{s}$ ) upon degassing the solution, we also assigned it to the triplet state. Although the presence of tellurium in **3** is responsible for a bathochromic shift of its emission band maximum compared to those of **1** and **2** (Figure 2), the

shift is not apparent in the transient spectra (Figures S9 and S10;  $\lambda_{\text{max}} = 437$  and  $\sim 620$  nm). The rate constants of the triplet decay ( $k_d^T$ ) in aerated and degassed solutions are also shown in Table 3.

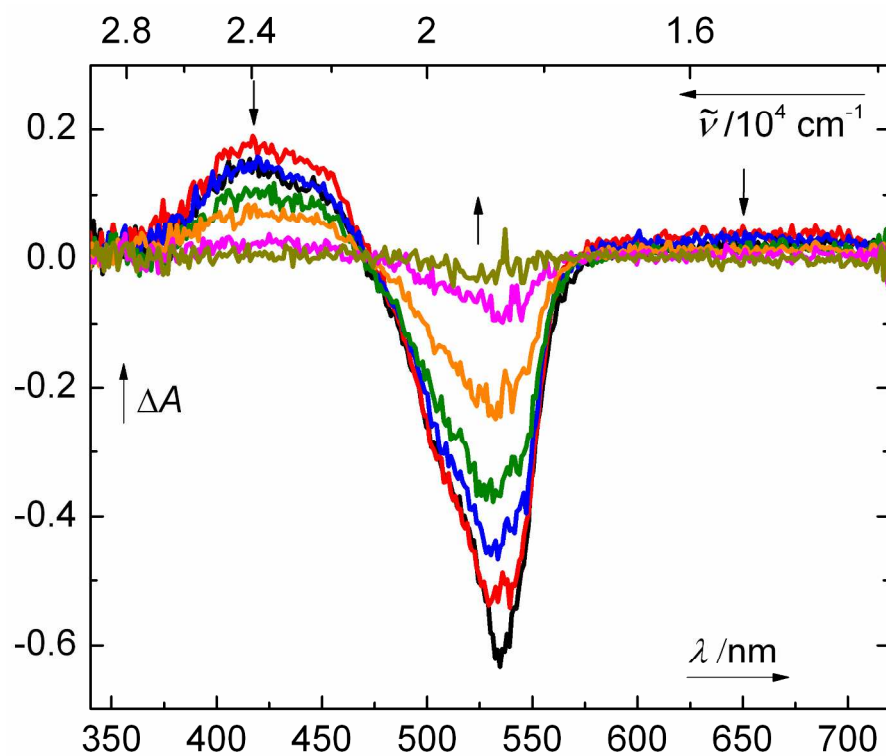


**Figure 3:** Transient spectra ( $\lambda_{\text{exc}} = 532$  nm) of **1** in non-degassed acetonitrile ( $c = 1.10 \times 10^{-5}$  mol dm $^{-3}$ ) obtained 8 ns–1  $\mu$ s after excitation (black: 8 ns; red: 20 ns; blue: 50 ns; green: 100 ns; orange: 200 ns; magenta: 500 ns; dark yellow: 1  $\mu$ s).

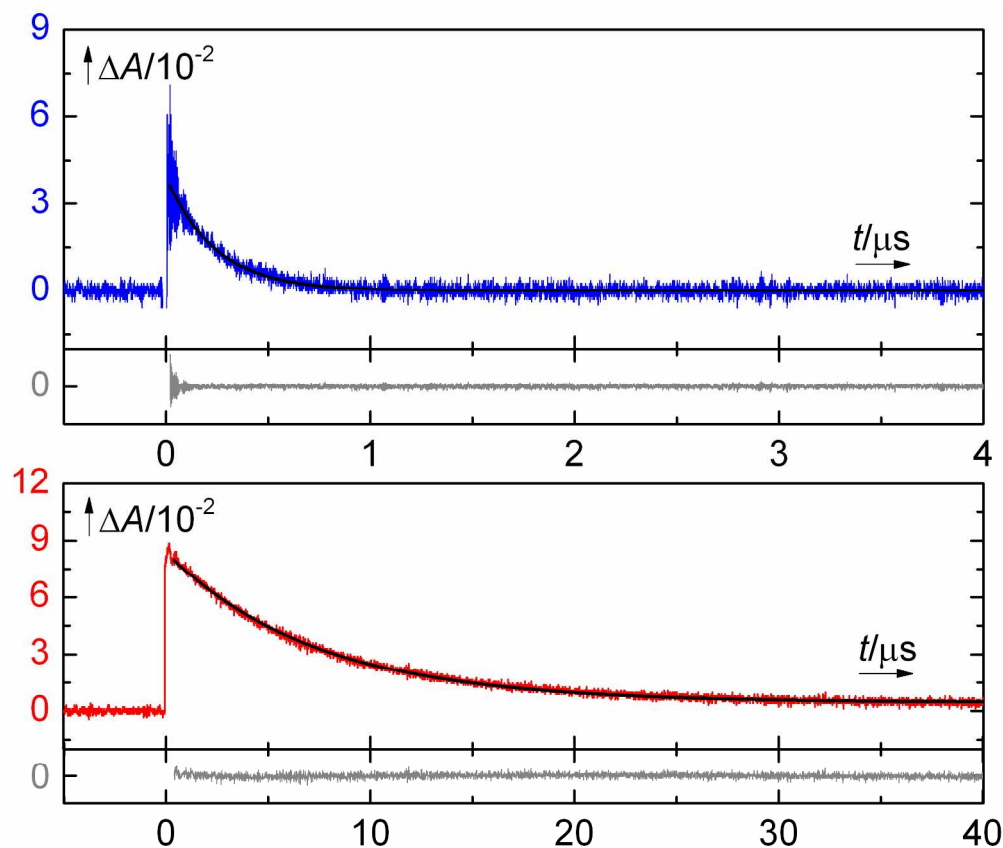


**Figure 4.** Representative kinetic traces and the residuals of a single-exponential fit of the signal for **1** excited at  $\lambda_{\text{exc}} = 532$  nm in aerated (top, kinetic trace: blue, exponential fit: black, sum of the residuals: gray) and degassed (bottom; kinetic trace: red, exponential fit: black, sum of the residuals: gray) acetonitrile ( $c = 1.10 \times 10^{-5}$  mol dm $^{-3}$ ) obtained at  $\lambda = 650$  nm (top) and  $\lambda = 420$  nm (bottom).

**Table 3.** Transient Absorption Data for **1–4**.

compd <sup>a</sup>	$\lambda_{\text{exc}}/\text{nm}^b$	cond <sup>c</sup>	$k_d^T/\text{s}^{-1}{}^d$	$\Phi_{\text{ISC}}^e$	$1-(\Phi_I+\Phi_{\text{ISC}})$	$\lambda_{\text{max}}^T/\text{nm}^f$	$\mathcal{E}_{\text{max}}^T{}^g$
<b>1</b>	532	deg	$(1.4 \pm 0.1) \times 10^5$	$0.40 \pm 0.02$	0.54	418	$16400 \pm 1700$
		air	$(4.2 \pm 0.2) \times 10^6$				
<b>2</b>	532	deg	$(1.4 \pm 0.1) \times 10^5$	$0.44 \pm 0.02$	0.36	435	$6500 \pm 500$
		air	$(4.3 \pm 0.1) \times 10^6$				
<b>3</b>	532	deg	$(1.2 \pm 0.1) \times 10^5$	$0.59 \pm 0.02$	0.31	437	$9900 \pm 800$
		air	$(4.2 \pm 0.2) \times 10^6$				
<b>4</b>	355	deg	$(1.4 \pm 0.1) \times 10^5$	$0.54 \pm 0.03$	0.31	417	$11800 \pm 1300$
		air	$(4.4 \pm 0.1) \times 10^6$				

<sup>a</sup> Solutions in acetonitrile: **1–3**:  $c = \sim 1.5 \times 10^{-5}$  mol dm $^{-3}$ ; **4**:  $c = \sim 4.5 \times 10^{-5}$  mol dm $^{-3}$ . <sup>b</sup> Laser pulses of  $\leq 170$  ps;  $E_{\text{pulse}} = 240$  mJ at  $\lambda_{\text{exc}} = 532$  nm or  $E_{\text{pulse}} = 160$  mJ at  $\lambda_{\text{exc}} = 355$  nm. <sup>c</sup> deg: degassed; air: aerated. <sup>d</sup> Rate constants of the triplet decay; a monoexponential fit based on 6

measurements. <sup>e</sup> Quantum yields of intersystem crossing (determined by a previously published method<sup>36</sup>), averaged from  $\geq 6$  measurements. <sup>f</sup> The maximum of triplet-triplet absorption and <sup>g</sup> its molar absorption coefficient,  $\epsilon_{\max}^T / \text{mol}^{-1} \text{ dm}^3 \text{ cm}^{-1}$  (the standard deviation was calculated from  $\geq 6$  independent measurements).

The reference 3-iodo BODIPY derivative **4**<sup>32</sup> does not absorb at 532 nm; therefore, 355-nm excitation was used for the transient spectroscopy measurements (Figures S11 and S12). The triplet spectrum possessed similar absorption peaks ( $\lambda_{\max}^T = 417$  and 667 nm) as those of **1–3**. The ground state bleach is masked by a high absorption of **4** in the region of 450–500 nm. We also attempted to investigate the model compounds **5** (no heavy atom) and **7** (Cl-atom containing derivative). However, we did not observe any triplet transient under the same experimental conditions, which points to a significantly lower ISC quantum yield (Figure S13).

Table 3 shows that the compounds **1–4** possess nearly identical triplet lifetimes (7–8 and 0.2  $\mu\text{s}$  for degassed and aerated acetonitrile solutions, respectively) and efficient ISC quantum yields ( $\Phi_{\text{ISC}} = 0.4–0.6$ ). The superimposed transient spectra of **1–4** obtained at 2 ns after the excitation are shown in Figure 5. The molar absorption coefficients were calculated using the Lambert-Beer law from  $\Delta A$  of the ground state bleach signal taken at 2 ns after excitation and a cuvette optical pathway determined using a solution of eosin Y as a standard ( $c = 1 \times 10^{-5} \text{ mol dm}^{-3}$ ; see Supporting Information). Compound **1** had the highest molar absorption coefficient at  $\lambda_{\max}$  in both the triplet-triplet (Table 3) and  $S_0 \rightarrow S_1$  absorption (Table 1) spectra. The shape of the ground state bleach of **4** differs somewhat from its absorption spectrum, which indicates that the triplet state partially absorbs in the region of 440–480 nm.

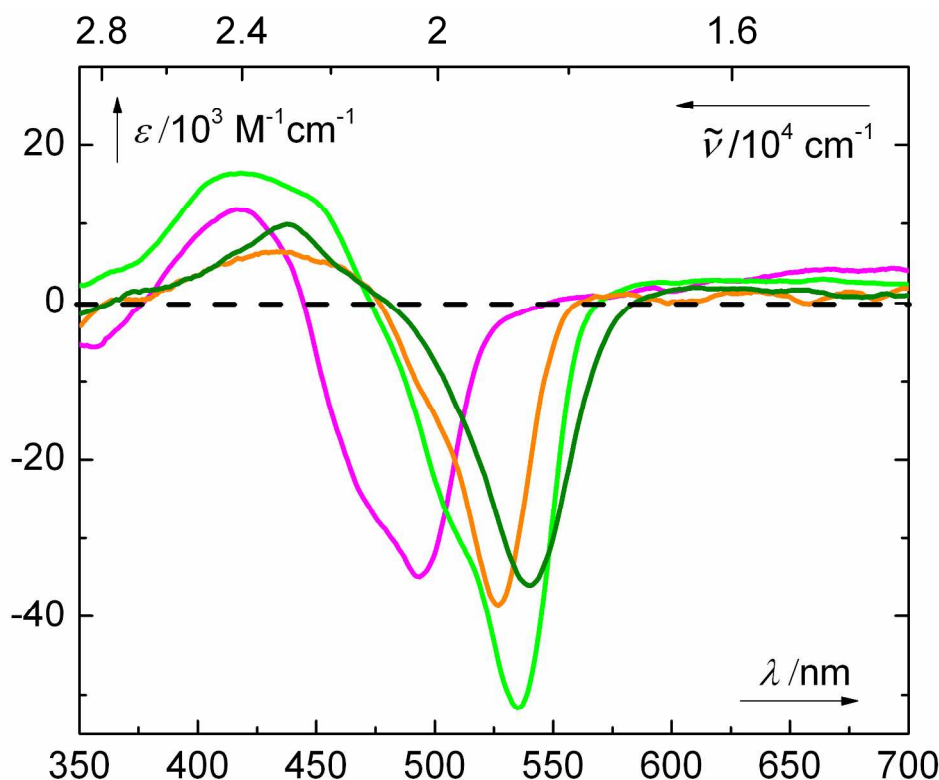


**Figure 5.** Transient spectra ( $\lambda_{\text{exc}} = 532 \text{ nm}$ ) of **1–4** in aerated acetonitrile solutions obtained at 2 ns after the excitation (the molar absorption coefficients are shown; **1**: light green; **2**: orange; **3**: dark green; **4**: magenta). The spectra were smoothed using a Savitzky-Golay algorithm; the untreated spectra are shown in Figure S14.

## Discussion

The aim of this work was to design and study BODIPY derivatives that exhibit efficient ISC as a consequence of the internal heavy-atom effect.<sup>12</sup> This effect is a short-distance phenomenon. For example, installation of the iodine atom to the *para*-position of the *meso*-phenyl group of BODIPY does not prevent its fluorescence;<sup>37</sup> however, when iodine is attached directly to the chromophore core, ISC becomes dominant.<sup>35</sup> In contrast, 2-iodothieryl BODIPY derivatives have been introduced as efficient triplet photosensitizers due to an extended  $\pi$ -conjugation of the 2-iodothieryl and BODIPY moieties.<sup>38</sup> Several heavy-atom-containing BODIPY derivatives have already been made and studied. Iodine-substituted derivatives indeed possess high ISC quantum yields but the compounds were found to be rather photolabile and induce cytotoxicity upon photoproduct formation.<sup>5, 10</sup> Only two studies have introduced Se- or Te-substituted BODIPY derivatives,<sup>30, 31</sup> and the effect of heavy atoms on the ISC quantum yields have not been evaluated. Therefore, we prepared monosubstituted Se- and Te-atom containing derivatives

**1–3** to compare their photophysical properties to those of the iodo or chloro analogues **4**, **6** and **7** and an unsubstituted derivative **5**.

Alkyl groups at the *meso* position are known to have no special effect on the absorption and emission spectra.<sup>6</sup> However, the presence of a phenyl group in the *meso* position of BODIPY was found to decrease the fluorescence efficiency due to a more efficient radiationless decay induced by a ring rotation.<sup>39</sup> This group can also impose a considerable steric hindrance for substituents in the positions 1 and 7, which then enhances the fluorescence.<sup>40</sup> When we compared the properties of the *meso* H- and methyl-analogues **1** and **2**, the fluorescence efficiency increased for **2** compared to those of **1** by a factor of 3 (Table 1). Nevertheless, the photostability of **2** was ~4 times higher than of **1** (Table 2); therefore, the *meso* methyl group was installed in all remaining compounds studied (**3–5**). The Se and Te atoms were installed to the position 3 because the syntheses via nucleophilic substitution are straightforward<sup>41</sup> (unlike the positions 2 and 6 that bear the least positive charge and are rather susceptible to an electrophilic attack).<sup>6</sup> Finally, the model 2-iodo BODIPY analogue **4** was used because the synthetic protocol was readily available.<sup>32</sup>

The absorption and emission spectra of all compounds **1–7** in acetonitrile (Figures 1 and 2) possess characteristic features of the basic BODIPY chromophore.<sup>42</sup> A sharp peak and its shoulder in the absorption spectra is a manifestation of the allowed  $S_0 \rightarrow S_1$  transition of the delocalized  $\pi$ -conjugated system. Smaller molar absorption coefficients ( $35\text{--}55 \times 10^3 \text{ mol}^{-1} \text{ dm}^3 \text{ cm}^{-1}$ ) than those of unsubstituted symmetrical BODIPY derivatives ( $80\text{--}120 \times 10^3 \text{ mol}^{-1} \text{ dm}^3 \text{ cm}^{-1}$ )<sup>8</sup> are probably caused by an asymmetric substitution pattern, leading to charge separation between the pyrrole rings.<sup>40</sup> A second, less pronounced band observed in the region of 225–400 nm is attributed to the  $S_0 \rightarrow S_2$  transition. A bathochromic shift observed in both absorption and emission spectra in the order of the substituents H/Cl  $\rightarrow$  I  $\rightarrow$  Se  $\rightarrow$  Te (Figures 1 and 2) is clearly a consequence of an increasing electron-donating ability of the substituent. The relatively small Stokes shifts (10–45 nm or  $397\text{--}1224 \text{ cm}^{-1}$ ; Table 1) observed in all derivatives are related to the rigidity of the BODIPY system.

The fluorescence quantum yields decreased with the heavy-atom substitution; nevertheless, residual fluorescence was still detected (Table 1). The heavy-atom effect must be responsible for fluorescence quenching but also for shortening of the phosphorescence lifetimes.<sup>11</sup> Examples of compounds bearing the chalcogen atoms that exhibit enhanced ISC in various chromophores have already been reported. For example, furan, thiophene, selenophene, or tellurophene and their derivatives exhibited a linear correlation with the atomic spin-orbit constant of the corresponding chalcogen in the series of O  $\rightarrow$  S  $\rightarrow$  Se  $\rightarrow$  Te.<sup>43, 44</sup>

In most of the literature reports, indirect measurements of the quantum yield of singlet oxygen ( $^1\text{O}_2$ ) generation serves as a tool to determine the ISC efficiency in BODIPY derivatives.<sup>5</sup> In this work, we identified the triplet state and determined the triplet lifetimes and ISC quantum yields for all compounds using nanosecond transient absorption measurements (Table 3).

Unfortunately, we could not evaluate the rate constants of the triplet state formation because the process was too fast for our ns apparatus. Similar transient spectra of the BODIPY triplets have also been reported for several BODIPY derivatives containing Se, Te,<sup>30</sup> and I<sup>40</sup> atoms.

Churchill and coworkers provided evidence for the photoinduced electron transfer (PET) from a phenyl tellurium group attached to the BODIPY core (they reported that the fluorescence quantum yield increased from 0.06 to 0.2 when the Te atom was oxidized to the corresponding tellurium oxide) in their search for selective sensing of hypochlorite ion in aqueous solutions.<sup>23, 31</sup> As the sum of the quantum yields of fluorescence and ISC never reached 100% in compounds studied in this work (the  $1 - (\Phi_f + \Phi_{ISC})$  values in Table 3 provide an indication of how efficient non-radiative deactivations are), other (radiationless) processes must contribute to the overall excitation decay. It is possible that PET from the chalcogens<sup>45</sup> to the S<sub>1</sub> excited BODIPY core<sup>46</sup> in **1–3** competes with ISC. As expected, tellurium in **3** enhanced the triplet state more efficiently than selenium in the derivatives **1** and **2** and iodine in **4** (by a factor below 1.4), whereas the decay of the corresponding triplets was essentially the same for all degassed samples (~7 μs), perhaps due to competition of a radiationless process or a cleavage of the carbon–chalcogen bond from the triplet-state manifold. As the data in Table 2 indicate, such a photochemical reductive chalcogen atom substitution (i.e., formation of the products **5** and **8**) must be one of the deexcitation channels. As a 2<sup>nd</sup> order kinetic model could not be fitted with the experimental data (see the Experimental Part and Supporting Information, page S35), triplet-triplet annihilation or self-quenching processes were excluded in our experiments.

Finally, if the applicability of the compounds **1–3** as triplet sensitizers is considered, all derivatives have the same magnitude of  $\Phi_{ISC}$  but their photostability is profoundly different (Table 2). The Te-atom substituted BODIPY is photochemically rather unstable, whereas the Se-derivative **2** exhibits a very high photochemical stability; its half-life under the identical irradiation conditions is almost two orders of magnitude longer than that of the 2-iodo BODIPY derivative **4**.

## Conclusions

Steady-state and transient spectroscopy studies of three novel monosubstituted 3-phenylselenanyl and 3-phenyltellanyl BODIPY derivatives were used to evaluate the extent of intersystem crossing related to the heavy-atom effect of the Se and Te atoms. It was found that its magnitude is comparable to that of the corresponding monosubstituted 2-iodo derivative. As the photostability of the selenium atom-containing derivatives was found relatively high, they could be considered as triplet sensitizers in various applications.

## Experimental Part

**Material and Methods.** The reagents and solvents of the highest purity available were used as purchased, or they were purified/dried using standard procedures and kept over activated 3 Å molecular sieves (8–12 mesh) under dry N<sub>2</sub>. The synthetic steps were performed under ambient atmosphere unless stated otherwise. The following synthetic intermediates, 5-chloro-1*H*-pyrrole-2-carbaldehyde, 1-(5-chloro-1*H*-pyrrol-2-yl)ethanone, 1-(4-iodo-1*H*-pyrrol-2-yl)ethanone, were synthesized using the procedure reported before.<sup>32</sup> All glassware was oven-dried prior to use. All purification procedures were performed using silica gel column or preparative thin layer chromatography.

<sup>1</sup>H and <sup>13</sup>C NMR spectra were recorded on 300 or 500 MHz spectrometers in chloroform-*d*, acetone-*d*<sub>6</sub>, or dichloromethane-*d*<sub>2</sub>. The NMR signals were referenced to the residual peak of the (major) solvent. The deuterated solvents were kept over activated 3 Å molecular sieves (8–12 mesh) under dry N<sub>2</sub>. UV absorption spectra and the molar absorption coefficients were obtained on a UV-vis spectrometer with matched 1.0-cm quartz cells. Fluorescence spectra were recorded on an automated luminescence spectrometer in 1.0 cm quartz fluorescence cuvettes at 25 ± 1 °C; the sample concentration was set to keep the absorbance below 0.1 at λ<sub>max</sub>; each sample was measured five times and the spectra were averaged. Emission and excitation spectra are normalized; they were corrected using standard correction files. A nanosecond flash lamp (filled with H<sub>2</sub>) was used for measuring the fluorescence lifetimes. The data obtained were deconvolved from the measured decay curves of the sample and the instrumental response function. HPLC (a reverse phase column C-8; UV and fluorescence detectors) was used to check the purity of the final synthetic products. Exact masses were obtained using a triple quadrupole electrospray ionization mass spectrometer in positive or negative ion mode. The melting points were determined on a non-calibrated Kofler's hot stage or in open-end capillary tubes using a non-calibrated melting point apparatus.

The nanosecond laser flash photolysis (LFP) setup was operated in a right-angle arrangement of the pump and probe beams. Laser pulses of 170 ps duration at 532 nm (240 mJ; the compounds **1–3**) or at 355 nm (160 mJ; the compound **4**) were obtained from a Nd:YAG laser. The laser beam was dispersed on a 40 mm long and 10 mm wide modified fluorescence cuvette (a 40 mm optical path). The probe light from a xenon lamp was filtered as necessary. The full description of the apparatus has been published before.<sup>47</sup> The measurements were performed at ambient temperature (20 ± 2 °C). Kinetic traces were fitted using a Levenberg-Marquard algorithm. All measurements were performed at least three times unless stated otherwise. All samples were irradiated by a single laser flash (all BODIPY derivatives are photoactive); the cuvette was filled with a fresh solution after each measurement. The samples were degassed by purging the solutions with oxygen-free nitrogen for 20 minutes in a modified Schlenk fluorescence quartz cuvette. Our degassing method was compared with a freeze-pump-thaw technique (3 cycles): the triplet lifetimes determined by both methods did not differ by more than 5%. In addition, the

procedure is highly reproducible as can be seen from standard deviations for the measured triplet lifetimes (Table 3).

**General Procedure for the Synthesis of the Compounds 4-7.** The synthesis was accomplished according to the reported procedure.<sup>32</sup> A solution of POCl<sub>3</sub> (1.1 equiv.) was added into a stirred solution of 1-(5-halo-1*H*-pyrrol-2-yl)ethanone derivative (1 equiv.) in chloroform (50 mL) (Scheme 1). The reaction mixture was stirred at 23 °C for 1 h. 2,4-Dimethyl-1*H*-pyrrole (1.1 equiv.) was added in to the reaction mixture which was further stirred at room temperature overnight. Triethylamine (1.1 equiv.) was then added to the solution and followed by the addition of BF<sub>3</sub>·Et<sub>2</sub>O (1.1 equiv.). The reaction mixture was stirred for 2.5 h. The reaction mixture was quenched with 10% of HCl (10 mL) and extracted with ethyl acetate. The organic layer was washed with water (3 × 10 mL), dried over MgSO<sub>4</sub> and filtered. The solvent was removed under reduced pressure. Column chromatography was used to purify the title compounds.

**Synthesis of 2-Iodo-4,4-difluoro-5,7,8-trimethyl-4-bora-3a,4a-diaza-*s*-indacene (4).** The following starting material was used: 1-(4-iodo-1*H*-pyrrol-2-yl)ethanone (500 mg, 2.13 mmol), POCl<sub>3</sub> (360 mg, 0.21 mL, 2.34 mmol), 2,4-dimethyl-1*H*-pyrrole (223 mg, 0.23 mL, 2.34 mmol), triethylamine (236 g, 0.32 mL, 2.34 mmol), BF<sub>3</sub>·Et<sub>2</sub>O (332 mg, 0.30 mL, 2.34 mmol). Column chromatography: silica gel; *n*-hexane/dichloromethane, 1 : 1, v/v. Orange solid. Yield: 500 mg (65%). <sup>1</sup>H NMR (500 MHz, acetone-*d*<sub>6</sub>): δ (ppm) 7.54 (s, 1H), 7.37 (s, 1H), 6.43 (s, 1H), 2.64 (s, 3H), 2.54 (s, 3H), 2.49 (s, 3H). The compound was characterized elsewhere.<sup>32</sup>

**Synthesis of 4,4-Difluoro-5,7,8-trimethyl-4-bora-3a,4a-diaza-*s*-indacene (5).** The following starting material was used: 1-(1*H*-pyrrol-2-yl)ethanone (100 mg, 0.92 mmol), POCl<sub>3</sub> (169 mg, 0.10 mL, 1.10 mmol), 2,4-dimethyl-1*H*-pyrrole (105 mg, 0.11 mL, 1.10 mmol), triethylamine (111 mg, 0.15 mL, 1.10 mmol), BF<sub>3</sub>·Et<sub>2</sub>O (156 mg, 0.14 mL, 1.10 mmol). Column chromatography: silica gel; *n*-hexane/dichloromethane, 6 : 4, v/v). Mp 163–164 °C. Orange solid. Yield: 29 mg (14%). <sup>1</sup>H NMR (500 MHz, CD<sub>2</sub>Cl<sub>2</sub>): δ (ppm) 7.56 (s, 1H), 7.14 (s, 1H), 6.45 (s, 1H), 6.21 (s, 1H), 2.59 (s, 3H), 2.54 (s, 3H), 2.44 (s, 3H). <sup>13</sup>C NMR (126 MHz, CD<sub>2</sub>Cl<sub>2</sub>): δ (ppm) 160.9, 146.7, 143.0, 138.0, 134.9, 134.8, 124.3, 123.5, 116.0, 17.27, 17.0, 15.2. HRMS (APCI) *m/z*: [M – H]<sup>–</sup> calcd. for C<sub>12</sub>H<sub>13</sub>BF<sub>2</sub>N<sub>2</sub> 233.1069; found 233.1067.

**Synthesis of 3-Chloro-4,4-difluoro-5,7-dimethyl-4-bora-3a,4a-diaza-*s*-indacene (6).** The following starting material was used: 5-chloro-1*H*-pyrrole-2-carbaldehyde (500 mg, 3.86 mmol), POCl<sub>3</sub> (651 mg, 0.40 mL, 4.2 mmol), 2,4-dimethyl-1*H*-pyrrole (400 mg, 0.44 mL, 4.2 mmol), triethylamine (427 mg, 0.59 mL, 4.2 mmol), BF<sub>3</sub>·Et<sub>2</sub>O (0.60 g, 0.52 mL, 4.2 mmol). Column chromatography: silica gel; *n*-hexane/dichloromethane, 6 : 4, v/v. Red crimson solid. Yield: 400 mg (40%). <sup>1</sup>H NMR (500 MHz, CD<sub>2</sub>Cl<sub>2</sub>): δ (ppm) 7.16 (s, 1H), 6.94 (d, 1H, *J* = 4.0 Hz), 6.35 (d, 1H, *J* = 4.0 Hz), 6.26 (s, 1H), 2.61 (s, 3H), 2.31 (s, 3H). The compound was characterized elsewhere.<sup>32</sup>

**Synthesis of 3-Chloro-4,4-difluoro-5,7,8-dimethyl-4-bora-3a,4a-diaza-s-indacene (7).** The following starting material was used: 1-(5-chloro-1*H*-pyrrol-2-yl)ethanone (500 mg, 3.48 mmol), POCl<sub>3</sub> (593 mg, 0.36 mL, 3.83 mmol), 2,4-dimethyl-1*H*-pyrrole (364 mg, 0.40 mL, 3.83 mmol), triethylamine (389 mg, 0.54 mL, 3.83 mmol), BF<sub>3</sub>·Et<sub>2</sub>O (550 mg, 0.47 mL, 3.83 mmol). Column chromatography: silica gel; *n*-hexane/dichloromethane, 6 : 4, v/v. Red crimson solid. Yield: 550 mg (59%). <sup>1</sup>H NMR (300 MHz, CDCl<sub>3</sub>): δ (ppm) 7.03 (d, 1H, J=3.63 Hz), 6.29 (d, 1H, J=3.66 Hz), 6.17 (s, 1H), 2.58 (s, 3H), 2.50 (s, 3H), 2.40 (s, 3H). The compound was characterized elsewhere.<sup>32</sup>

**General Procedure for the Synthesis of the Compounds 1 and 2.** This synthesis is a modification of the method Vosch and coworkers (Scheme 1).<sup>30</sup> A BODIPY precursor (1 molar equiv.) was added to a solution of benzeneselenol (1.5 equiv.) and Cs<sub>2</sub>CO<sub>3</sub> (1.5 equiv.) in dry acetonitrile under nitrogen atmosphere, and the reaction mixture was stirred at 20 °C. After disappearance of the starting material (TLC; ~10 min), water was added and the crude product was extracted with dichloromethane. The organic phases were dried over MgSO<sub>4</sub>, filtered and concentrated to dryness. The resulting product was purified by preparative TLC (silica gel; *n*-hexane/ethyl acetate, 8 : 2, v/v).

**Synthesis of 3-Phenylselanyl-4,4-difluoro-5,7-dimethyl-4-bora-3a,4a-diaza-s-indacene (1).** The following starting material was used: **6** (50 mg, 0.20 mmol), benzeneselenol (46 mg, 31.3 μL, 0.29 mmol) and Cs<sub>2</sub>CO<sub>3</sub> (96 mg, 0.29 mmol), and dry acetonitrile (10 mL). Red solid. Yield: 50 mg (67%). Mp 145–146 °C. <sup>1</sup>H NMR (500 MHz, CD<sub>2</sub>Cl<sub>2</sub>): δ (ppm) 7.74 (m, 2H), 7.43 (m, 3H), 7.07 (s, 1H), 6.82 (d, 1H, J=4.1 Hz), 6.15 (s, 1H), 5.90 (d, 1H, J = 4.1 Hz), 2.54 (s, 3H), 2.25 (s, 3H). <sup>13</sup>C NMR (126 MHz, CD<sub>2</sub>Cl<sub>2</sub>): δ (ppm) 159.8, 149.6, 143.5, 136.1, 136.0, 135.2, 129.7, 129.3, 127.4, 126.84, 126.83, 126.81, 121.6, 120.2, 119.6, 14.7, 11.1. HRMS (APCI<sup>+</sup>) *m/z*: [M + H]<sup>+</sup> calcd. for C<sub>17</sub>H<sub>15</sub>BF<sub>2</sub>N<sub>2</sub>Se 377.0538; found 377.0536.

**Synthesis of 3-Phenylselanyl-4,4-difluoro-5,7,8-trimethyl-4-bora-3a,4a-diaza-s-indacene (2).** The following starting material was used: **7** (40 mg, 0.15 mmol), benzeneselenol (34.9 mg, 23.7 μL, 0.22 mmol), Cs<sub>2</sub>CO<sub>3</sub> (72.8 mg, 0.22 mmol), dry acetonitrile (10 mL). Dark red solid. Yield: 38 mg (60%). Mp 151–152 °C. <sup>1</sup>H NMR (500 MHz, CD<sub>2</sub>Cl<sub>2</sub>): δ (ppm) 7.73 (m, 2H), 7.42 (m, 3H), 7.02 (d, 1H, J = 4.2 Hz), 6.17 (s, 1H), 5.94 (d, 1H, J = 4.2 Hz), 2.54 (s, 3H), 2.49 (s, 3H), 2.41 (s, 3H). <sup>13</sup>C NMR (126 MHz, CD<sub>2</sub>Cl<sub>2</sub>): δ (ppm) 158.0, 157.6, 147.5, 144.2, 139.7, 139.5, 137.7, 136.5, 133.9, 130.2, 129.7, 127.9, 125.5, 122.6, 119.7, 17.0, 16.6, 15.1. HRMS (APCI<sup>+</sup>) *m/z*: [M + H]<sup>+</sup> calcd. for C<sub>18</sub>H<sub>17</sub>BF<sub>2</sub>N<sub>2</sub>Se 391.0695; found 391.0694.

**Synthesis of 3-Phenyltellanyl-4,4-difluoro-5,7,8-trimethyl-4-bora-3a,4a-diaza-s-indacene (3).** The synthesis was accomplished according to the method reported by Vosch and coworkers (Scheme 1).<sup>30</sup> The solution of sodium borohydride (40 mg, 1.06 mmol) in ethanol (4 mL) was slowly added to the solution of diphenyl ditelluride (91.5 mg, 0.22 mmol) in ethanol (4 mL) under nitrogen atmosphere until the solution became nearly colorless. The resulting solution was immediately transferred to the solution of the chloride **7** (40 mg, 0.15 mmol) in dry

tetrahydrofuran (10 mL). The reaction mixture was stirred at room temperature under nitrogen atmosphere for 12 h. The resulting solution was extracted with dichloromethane (3×15 mL) and the organic layer was dried over MgSO<sub>4</sub>. The solvent was removed under reduced pressure, and the crude was purified by preparative TLC (silica gel GF254; *n*-hexane/EtOAc, 8 : 2, v/v). Violet solid. Yield: 45 mg (68%). Mp 131–132 °C. <sup>1</sup>H NMR (500 MHz, acetone-*d*<sub>6</sub>): δ (ppm) 8.00 (m, 2H), 7.44 (m, 3H), 7.20 (d, 1H, *J* = 4.0 Hz), 6.26 (s, 1H), 6.00 (d, 1H, *J* = 4.0 Hz), 2.57 (s, 3H), 2.51 (s, 3H), 2.44 (s, 3H). <sup>13</sup>C NMR (126 MHz, acetone-*d*<sub>6</sub>): δ (ppm) 157.7, 144.7, 141.9, 140.2, 140.1, 134.2, 132.3, 130.7, 130.2, 126.3, 124.2, 122.7, 113.65, 113.61, 113.58, 16.6, 16.3, 14.7. HRMS (APCI<sup>+</sup>) *m/z*: [M + H]<sup>+</sup> calcd. for C<sub>18</sub>H<sub>17</sub>BF<sub>2</sub>N<sub>2</sub>Te 441.0592; found 441.0591.

**Stability of the BODIPY Derivatives in the Dark.** A freshly prepared solution of the corresponding compound in spectroscopic-grade acetonitrile ( $c = 1\text{--}3 \times 10^{-5}$  mol dm<sup>-3</sup>) in a 1 cm quartz cuvette was left in the dark at 23 °C, while UV-vis absorption spectra were periodically recorded using a diode-array spectrophotometer. The concentration changes of the compounds were calculated using the molar absorption coefficients.

**Photochemical Stability of the BODIPY Derivatives.** A freshly prepared solution of the corresponding compound in spectroscopic-grade acetonitrile ( $c = 1\text{--}3 \times 10^{-5}$  mol dm<sup>-3</sup>) in a 1 cm quartz cuvette was irradiated with a home-made device equipped with 32 high-energy LEDs (100 mW) emitting at  $\lambda_{\text{em}} = 525 \pm 11$  nm at the distance of ~1 cm from the cuvette window. The reaction progress was monitored using a diode-array UV-vis spectrophotometer. The half-lives of the compounds were calculated from a plot of the absorbance at  $\lambda_{\text{irrad}}$  against time by fitting the data to a pseudo-first order kinetic equation. The relative half-lives ( $\tau_{1/2}$ ) in Table 2 were recalculated for the same initial sample absorbance.

**Determination of the Intersystem Crossing Quantum Yields.** The intersystem crossing quantum yields were calculated from the relative ratios of the areas of the absorption and ground state bleach bands in the transient spectrum. Both spectra were obtained with fresh samples under the same experimental conditions, and the measurements were repeated at least six times. The absorbance of 0.1 at the wavelength of excitation was retained to minimize the interference of the ground state absorption. The light-saturation conditions were kept for all measurements. The sample concentrations and the laser energy were chosen to ensure that the decay of the triplets was first order, thus self-quenching as well as triplet-triplet annihilation processes were negligible (for details see Supporting Information, page S35).

A step-by-step procedure of the ISC quantum yield determination and the method optimization are provided in the Supporting Information (page S39). In addition, the reliability of this procedure was confirmed by a well-established reference method for determination of the ISC quantum yield reported by Das and coworkers using β-carotene as a triplet quencher (Table S1).<sup>48</sup>

## Acknowledgement

This project was supported by the National Sustainability Programme of the Czech Ministry of Education, Youth and Sports (LO1214) and the RECETOX research infrastructure (LM2011028). The authors thank Jakob Wirz for fruitful discussions.

## References

1. A. C. Benniston, G. Copley, Lighting the way ahead with boron dipyrromethene (BODIPY) dyes, *Phys. Chem. Chem. Phys.*, 2009, **11**, 4124-4131.
2. M. Benstead, G. H. Mehl, R. W. Boyle, 4,4'-Difluoro-4-bora-3a,4a-diaza-*s*-indacenes (BODIPYs) as components of novel light active materials, *Tetrahedron*, 2011, **67**, 3573-3601.
3. A. Bessette, G. S. Hanan, Design, synthesis and photophysical studies of dipyrromethene-based materials: insights into their applications in organic photovoltaic devices, *Chem. Soc. Rev.*, 2014, **43**, 3342-3405.
4. N. Boens, V. Leen, W. Dehaen, Fluorescent indicators based on BODIPY, *Chem. Soc. Rev.*, 2012, **41**, 1130-1172.
5. A. Kamkaew, S. H. Lim, H. B. Lee, L. V. Kiew, L. Y. Chung, K. Burgess, BODIPY dyes in photodynamic therapy, *Chem. Soc. Rev.*, 2013, **42**, 77-88.
6. A. Loudet, K. Burgess, BODIPY dyes and their derivatives: Syntheses and spectroscopic properties, *Chem. Rev.*, 2007, **107**, 4891-4932.
7. H. Lu, J. Mack, Y. C. Yang, Z. Shen, Structural modification strategies for the rational design of red/NIR region BODIPYs, *Chem. Soc. Rev.*, 2014, **43**, 4778-4823.
8. G. Ulrich, R. Ziessel, A. Harriman, The chemistry of fluorescent bodipy dyes: Versatility unsurpassed, *Angew. Chem. Int. Ed.*, 2008, **47**, 1184-1201.
9. J. Z. Zhao, W. H. Wu, J. F. Sun, S. Guo, Triplet photosensitizers: from molecular design to applications, *Chem. Soc. Rev.*, 2013, **42**, 5323-5351.
10. T. Yogo, Y. Urano, Y. Ishitsuka, F. Maniwa, T. Nagano, Highly efficient and photostable photosensitizer based on BODIPY chromophore, *J. Am. Chem. Soc.*, 2005, **127**, 12162-12163.
11. P. Klan, J. Wirz, *Photochemistry of organic compounds: From concepts to practice*, John Wiley & Sons Ltd., Chichester, 2009.
12. K. N. Solovyov, E. A. Borisevich, Intramolecular heavy-atom effect in the photophysics of organic molecules, *Phys. Usp.*, 2005, **48**, 231-253.
13. M. Galletta, S. Campagna, M. Quesada, G. Ulrich, R. Ziessel, The elusive phosphorescence of pyrromethene-BF<sub>2</sub> dyes revealed in new multicomponent species containing Ru(II)-terpyridine subunits, *Chem. Commun.*, 2005, 4222-4224.

14. A. A. Rachford, R. Ziessel, T. Bura, P. Retailleau, F. N. Castellano, Boron Dipyrromethene (BODIPY) Phosphorescence Revealed in Ir(ppy)(2)(bpy-CC-Bodipy)<sup>+</sup>, *Inorg. Chem.*, 2010, **49**, 3730-3736.
15. S. H. Lim, C. Thivierge, P. Nowak-Sliwinska, J. Y. Han, H. van den Bergh, G. Wagnieres, K. Burgess, H. B. Lee, In vitro and in vivo photocytotoxicity of boron dipyrromethene derivatives for photodynamic therapy, *J. Med. Chem.*, 2010, **53**, 2865-2874.
16. W. H. Wu, H. M. Guo, W. T. Wu, S. M. Ji, J. Z. Zhao, Organic triplet sensitizer library derived from a single chromophore (BODIPY) with long-lived triplet excited state for triplet-triplet annihilation based upconversion, *J. Org. Chem.*, 2011, **76**, 7056-7064.
17. Y. Cakmak, S. Kolemen, S. Duman, Y. Dede, Y. Dolen, B. Kilic, Z. Kostereli, L. T. Yildirim, A. L. Dogan, D. Guc, E. U. Akkaya, Designing excited states: Theory-guided access to efficient photosensitizers for photodynamic action, *Angew. Chem. Int. Ed.*, 2011, **50**, 11937-11941.
18. S. Duman, Y. Cakmak, S. Kolemen, E. U. Akkaya, Y. Dede, Heavy atom free singlet oxygen generation: Doubly substituted configurations dominate S<sub>1</sub> states of bis-BODIPYs, *J. Org. Chem.*, 2012, **77**, 4516-4527.
19. M. Broring, R. Kruger, S. Link, C. Kleeberg, S. Kohler, X. Xie, B. Ventura, L. Flamigni, Bis(BF<sub>2</sub>)-2,2'-bidipyrins (BisBODIPYs): Highly fluorescent BODIPY dimers with large Stokes shifts, *Chem. Eur. J.*, 2008, **14**, 2976-2983.
20. B. Ventura, G. Marconi, M. Broring, R. Kruger, L. Flamigni, Bis(BF<sub>2</sub>)-2,2'-bidipyrins, a class of BODIPY dyes with new spectroscopic and photophysical properties, *New J. Chem.*, 2009, **33**, 428-438.
21. K. Konig, Multiphoton microscopy in life sciences, *J. Microsc.*, 2000, **200**, 83-104.
22. A. J. Mukherjee, S. S. Zade, H. B. Singh, R. B. Sunoj, Organoselenium chemistry: Role of intramolecular interactions, *Chem. Rev.*, 2010, **110**, 4357-4416.
23. S. T. Manjare, Y. Kim, D. G. Churchill, Selenium- and tellurium-containing fluorescent molecular probes for the detection of biologically important analytes, *Acc. Chem. Res.*, 2014, **47**, 2985-2998.
24. C. W. Nogueira, G. Zeni, J. B. T. Rocha, Organoselenium and organotellurium compounds: Toxicology and pharmacology, *Chem. Rev.*, 2004, **104**, 6255-6285.
25. B. Tang, Y. L. Xing, P. Li, N. Zhang, F. B. Yu, G. W. Yang, A rhodamine-based fluorescent probe containing a Se-N bond for detecting thiols and its application in living cells, *J. Am. Chem. Soc.*, 2007, **129**, 11666-11667.
26. Z. R. Lou, P. Li, X. F. Sun, S. Q. Yang, B. S. Wang, K. L. Han, A fluorescent probe for rapid detection of thiols and imaging of thiols reducing repair and H<sub>2</sub>O<sub>2</sub> oxidative stress cycles in living cells, *Chem. Commun.*, 2013, **49**, 391-393.
27. S. J. Balkrishna, A. S. Hodage, S. Kumar, P. Panini, Sensitive and regenerable organochalcogen probes for the colorimetric detection of thiols, *RSC Adv.*, 2014, **4**, 11535-11538.
28. B. S. Wang, P. Li, F. B. Yu, J. S. Chen, Z. J. Qu, K. L. Han, A near-infrared reversible and ratiometric fluorescent probe based on Se-BODIPY for the redox cycle mediated by hypobromous acid and hydrogen sulfide in living cells, *Chem. Commun.*, 2013, **49**, 5790-5792.

29. S. T. Manjare, S. Kim, W. Do Heo, D. G. Churchill, Selective and sensitive superoxide detection with a new diselenide-based molecular probe in living breast cancer cells, *Org. Lett.*, 2014, **16**, 410-412.
30. E. Fron, E. Coutino-Gonzalez, L. Pandey, M. Sliwa, M. Van der Auweraer, F. C. De Schryver, J. Thomas, Z. Y. Dong, V. Leen, M. Smet, W. Dehaen, T. Vosch, Synthesis and photophysical characterization of chalcogen substituted BODIPY dyes, *New J. Chem.*, 2009, **33**, 1490-1496.
31. S. T. Manjare, J. Kim, Y. Lee, D. G. Churchill, Facile *meso*-BODIPY annulation and selective sensing of hypochlorite in water, *Org. Lett.*, 2014, **16**, 520-523.
32. V. Leen, E. Braeken, K. Luckermans, C. Jackers, M. Van der Auweraer, N. Boens, W. Dehaen, A versatile, modular synthesis of monofunctionalized BODIPY dyes, *Chem. Commun.*, 2009, 4515-4517.
33. V. Leen, T. Leemans, N. Boens, W. Dehaen, 2- and 3-Monohalogenated BODIPY dyes and their functionalized analogues: Synthesis and spectroscopy, *Eur. J. Org. Chem.*, 2011, **2011**, 4386-4396.
34. M. Kollmannsberger, T. Gareis, S. Heintl, J. Breu, J. Daub, Electrogenated chemiluminescence and proton-dependent switching of fluorescence: Functionalized difluoroboradiaza-*s*-indacenes, *Angew. Chem. Int. Ed.*, 1997, **36**, 1333-1335.
35. X. F. Zhang, X. D. Yang, Singlet oxygen generation and triplet excited-state spectra of brominated BODIPY, *J. Chem. Phys. B*, 2013, **117**, 5533-5539.
36. R. Bonneau, I. Carmichael, G. L. Hug, Molar absorption coefficients of transient species in solution, *Pure Appl. Chem.*, 1991, **63**, 290-299.
37. C. Tahtaoui, C. Thomas, F. Rohmer, P. Klotz, G. Duportail, Y. Mely, D. Bonnet, M. Hibert, Convenient method to access new 4,4-dialkoxy- and 4,4-diaryloxy-diaza-*s*-indacene dyes: Synthesis and spectroscopic evaluation, *J. Org. Chem.*, 2007, **72**, 269-272.
38. Y. H. Chen, J. Z. Zhao, L. J. Xie, H. M. Guo, Q. T. Li, Thienyl-substituted BODIPYs with strong visible light-absorption and long-lived triplet excited states as organic triplet sensitizers for triplet-triplet annihilation upconversion, *RSC Adv.*, 2012, **2**, 3942-3953.
39. H. L. Kee, C. Kirmaier, L. H. Yu, P. Thamyongkit, W. J. Youngblood, M. E. Calder, L. Ramos, B. C. Noll, D. F. Bocian, W. R. Scheidt, R. R. Birge, J. S. Lindsey, D. Holten, Structural control of the photodynamics of boron-dipyrrin complexes, *J. Chem. Phys. B*, 2005, **109**, 20433-20443.
40. M. J. Ortiz, A. R. Agarrabeitia, G. Duran-Sampedro, J. B. Prieto, T. A. Lopez, W. A. Massad, H. A. Montejano, N. A. Garcia, I. L. Arbeloa, Synthesis and functionalization of new polyhalogenated BODIPY dyes. Study of their photophysical properties and singlet oxygen generation, *Tetrahedron*, 2012, **68**, 1153-1162.
41. V. Lakshmi, M. R. Rao, M. Ravikanth, Halogenated boron-dipyrrmethenes: synthesis, properties and applications, *Org. Biomol. Chem.*, 2015, **13**, 2501-2517.
42. T. Rohand, W. W. Qin, N. Boens, W. Dehaen, Palladium-catalyzed coupling reactions for the functionalization of BODIPY dyes with fluorescence spanning the visible spectrum, *Eur. J. Org. Chem.*, 2006, 4658-4663.
43. M. Zander, The intra-annular internal heavy-atom effect on the fluorescence and phosphorescence properties of oxygen, sulphur or selenium containing heterocyclic systems related to dibenzo[b,n]perylene, *Z. Naturforsch. A*, 1989, **44**, 1116-1118.

44. M. Zander, G. Kirsch, On the phosphorescence of benzologues of furan, thiophene, selenophene, and tellurophene. A systematic study of the intra-annular internal heavy-atom effect, *Z. Naturforsch. A*, 1989, **44**, 205-209.
45. Z. Shen, H. Rohr, K. Rurack, H. Uno, M. Spieles, B. Schulz, G. Reck, N. Ono, Boron-diindomethene (BDI) dyes and their tetrahydrobicyclo precursors - en route to a new class of highly emissive fluorophores for the red spectral range, *Chem. Eur. J.*, 2004, **10**, 4853-4871.
46. S. Hattori, K. Ohkubo, Y. Urano, H. Sunahara, T. Nagano, Y. Wada, N. V. Tkachenko, H. Lemmetyinen, S. Fukuzumi, Charge separation in a nonfluorescent donor-acceptor dyad derived from boron dipyrromethene dye, leading to photocurrent generation, *J. Chem. Phys. B*, 2005, **109**, 15368-15375.
47. L. Klicova, P. Sebej, T. Solomek, B. Hellrung, P. Slavicek, P. Klan, D. Heger, J. Wirz, Adiabatic triplet state tautomerization of *p*-hydroxyacetophenone in aqueous solution, *J. Phys. Chem. A*, 2012, **116**, 2935-2944.
48. C. V. Kumar, L. Qin, P. K. Das, Aromatic thioketone triplets and their quenching behaviour towards oxygen and di-*t*-butylnitroxyl radical. A laser-flash-photolysis study, *J. Chem. Soc., Faraday Trans. 2*, 1984, **80**, 783-793.